ELSEVIER

Active defense mechanisms of thorny catfish

Haocheng Quan [1], Wen Yang [2,3,*], Zixiang Tang [4], Robert O. Ritchie [3,5], Marc A. Meyers [1,2,4,*]

[1] Materials Science and Engineering Program, University of California, San Diego, CA 92093, USA
[2] Department of NanoEngineering, University of California, San Diego, CA 92093, USA
[3] Materials Sciences Division, Lawrence Berkeley National Laboratory, Berkeley, CA 94720, USA
[4] Department of Mechanical and Aerospace Engineering, University of California, San Diego, CA 92093, USA
[5] Department of Materials Science and Engineering, University of California, Berkeley, CA 94720, USA

The thorny catfish (Doradidae; order Siluriforme), has characteristic barbed pectoral fin spines and mid-lateral scutes that work in concert to provide an active mechanical defense mechanism. The pectoral spines can be locked into several fixed positions at angles between 0° and 90° to the longitudinal axis. Upon deployment they provide a formidable barrier to deglutition by a predator. Additionally, each spine contains two rows of sharp serrations which are inclined to its axis and can slice through tissue. We characterize the internal structure of the rotation joint of the pectoral spines and unravel the locking mechanism which is ensured by dual sources of friction generated from the dorsal and anterior components on the spine base. In addition to the lockable spines, thorny catfish also possess two arrays of mid-lateral dermal scutes with a sharp hook shape and gradient inner structure, which also have potential cutting capability and are part of the fish's active defense, since they can injure the predator through rapid motions of the catfish body. The structural design of these two weapons is very impressive, including a hollow structure, porous components, and gradient transitions, leading to outstanding performance by maintaining strength, toughness and light weight synergistically. These designs may provide inspiration for the development of novel structural materials or new armor materials.

Introduction

Through billions of years of evolution, the complexity of living organisms has kept increasing, driven in many cases by predator–prey interactions [1]. In order to survive, maintain the population, and keep the ecological balance, prey have developed various mechanisms of anti-predator adaptation. A variety of passive defense mechanisms, such as camouflage, nocturnality, playing dead, protective armor, and others are used for the purpose of avoiding detection or resisting attack. From the perspective of materials science, the natural flexible dermal/epidermal armors are an eloquent examples. They were developed by convergent evolution in mammals, reptiles and fish, and represent extraordinary structural designs with performance exceeding many synthetic materials at the same scale [2,3]. For example, the pangolin possesses overlapped scales which are mainly composed of keratin and fully cover its body (in the retracted position) for protection [4]. Armadillo, turtle, and fish evolved collagen-based bony plates, leather shells and scales, respectively, serving as dermal armors which are not only strong enough to resist the penetration by the teeth and claws of preda-

* Corresponding authors.
E-mail addresses: Yang, W. (wey005@eng.ucsd.edu), Meyers, M.A. (mameyers@eng.ucsd.edu).

 https://doi.org/10.1016/j.mattod.2020.04.028

tors, but also damage-tolerant through the deformability, enabled by the hierarchically assembled collagen [5–9] intermeshed with minerals. These natural materials with their intricate and ingenious structures provide inspiration for fabricating novel light-weight, strong and tough high-performance armors.

However, some organisms also adopt active defense mechanisms. Instead of waiting to be attacked by predators, they actively use their unique functional organs to assist them in escaping by means of, for example, poison release and threatening postures. Some of these active defense mechanisms are chemically based. For example, many marine mollusks, notably sea hares, cuttlefish, squid and octopus, release thick black ink to escape from the predators by scaring and distracting them [10]. Skunks (*Mephitis*) generate and spray out a liquid with very strong odor, using their anal glands, potent enough to discourage predators and even cause temporary blindness [11]. Some small animals, like sea cucumbers (*Holothuria forskali*), when irritated, can expel a few toxic Cuvierian tubules which lengthen, instantly become sticky, and can rapidly immobilize most predators with which they come into contact [12]. The hagfish [13] expels keratin filaments which form a hydrogel-like substance engulfing the predator's mouth. These active defense mechanisms rely mainly on the chemicals produced in glands by metabolism but cannot provide inspiration for load-bearing materials or novel structures.

There is another group of animals which have active defense mechanisms operating on mechanical principles. Hairy frogs (*Trichobatrachus robustus*) are compelling by their ability to break their erectile, terminal phalanges to inflict cuts in their antagonist's skin, forming sharp bony claws to fight against predators [14]. Similarly, the threatened Spanish ribbed newt (*Pleurodeles waltl*) can protrude its spear-shaped ribs through the body wall, forming sharp spines on the back to warn or stab the enemies [15]. More well-known examples are porcupines and hedgehogs, which possess sharp quills or spines covering their body. These quills and spines use the same design strategy; a thin keratinous cortex (shell) filled with closed-cell foam that is detachable and able to penetrate the skin of the predator. The architecture of quills and spines improves the compressive and flexure/buckling resistance while maintaining the light-weight [16–18].

Here we focus interest on two active anti-predatory mechanisms adapted, by catfish (*Siluriformes*), which have scarcely been noticed by materials scientists or structural engineers. The catfish has evolved a pair of stout pectoral fin spines which can be deployed (adducted) and retracted (abducted) repeatedly, producing stridulating sounds for intraspecies communication or to warn predators [19]. When threatened, the pair of spines can also be rigidly locked in the abducted position, which serves to increase its cross-sectional circumference to provide protection from predators with a limited gape, effectively making the catfish too big to swallow [20]. The cutting edges and serrations lining the spines add injury to the potential predator. Experimental evidence also proves that the presence of locked spines significantly increases the handling time, making preying on catfish an unfavorable choice [21]. There are reports of catfish spines being implicated in wounds or death of largemouth bass, water snakes, great egrets, and brown pelicans, proving that they are able to cut the soft tissue inside their predators [20]. Some catfish even have venom glands in the pectoral fin spines, causing additional harm to predators [22]. In addition to their pectoral spines, thorny catfish (*Siluriformes Doradidae*) have two sets of mid-lateral scute rows on both lateral sides of their body [23]. These bony thorns have a hooked shape and can also cause additional damage to the predators when the catfish flexes its body repeatedly, enhancing its chance to escape.

In this article, we reveal the dual friction-based locking mechanism of the pectoral spines in the thorny catfish and characterize the structure and mechanical properties of its spine and mid-lateral scutes. Our results uncover the active defense mechanisms of the armored catfish and can provide inspiration for the materials science or structural engineering community to create novel structural materials or new designs for armor materials.

Results

The thorny catfish studied, shown in Fig. 1a, was caught in the Paraguay River in southern Brazil. When the fish was taken out of water, a pair of sharp lateral fins, termed pectoral fin spines, were deployed and locked in their open (protective) position. The fish also had two arrays of sharp thorny scutes with hooked tips on both mid-lateral sides of its body for additional protection. These active defense mechanisms are now analyzed in the sections below.

Pectoral spines: locking mechanisms

After being sacrificed and skeletonized, the fish head with its pectoral and dorsal fin spines was separated from the body. Fig. 1b shows the pectoral spines that can be locked in several positions during the deploying (abductive) movement. We define locking here is as in certain positions, a distinct resistance force is generated to resist further opening (abductive) or closing (adductive) of the spines; the lock can only be released when an appropriate torque applied. This locking phenomenon of the abduction/adduction motion occurs in the skeleton with the soft tissues (muscle and tendon) assisting in the immobilization by bringing the components together and promoting the frictional force between them. The locking (or resistant) force is produced by pushing the components together and allowing the friction between bony surfaces to operate. It relies on the complex articulation formed by the spine base with the bones of the pectoral girdle, as shown in Fig. 1c. The rotation of the spine occurs in a channel (also called fossa) in a cam-like mechanism. Fig. 2 provides images of the detailed structures of the spine base and pectoral girdle.

The isolated girdle in Fig. 2a is split along the dotted line in the image to display its inner structural features. The two separate parts of the girdle, shown in Fig. 2b, reveal the two structural elements in the locking system. Micro-computerized tomography (micro-CT) of the cavernous structure (Fig. 2c) in the dashed box (left side of Fig. 2b), also referred to as the locking chamber (fossa) [24], reveals that it comprises a concave chamber with an internal rough surface. The other part of girdle, shown on the right in Fig. 2b, contains another key element - the spinal channel (fossa), which is contained within the black dotted line boxes on the right. Its detailed structure (Fig. 2d) indicates that the inner lateral wall of the channel has numerous highly mineral-

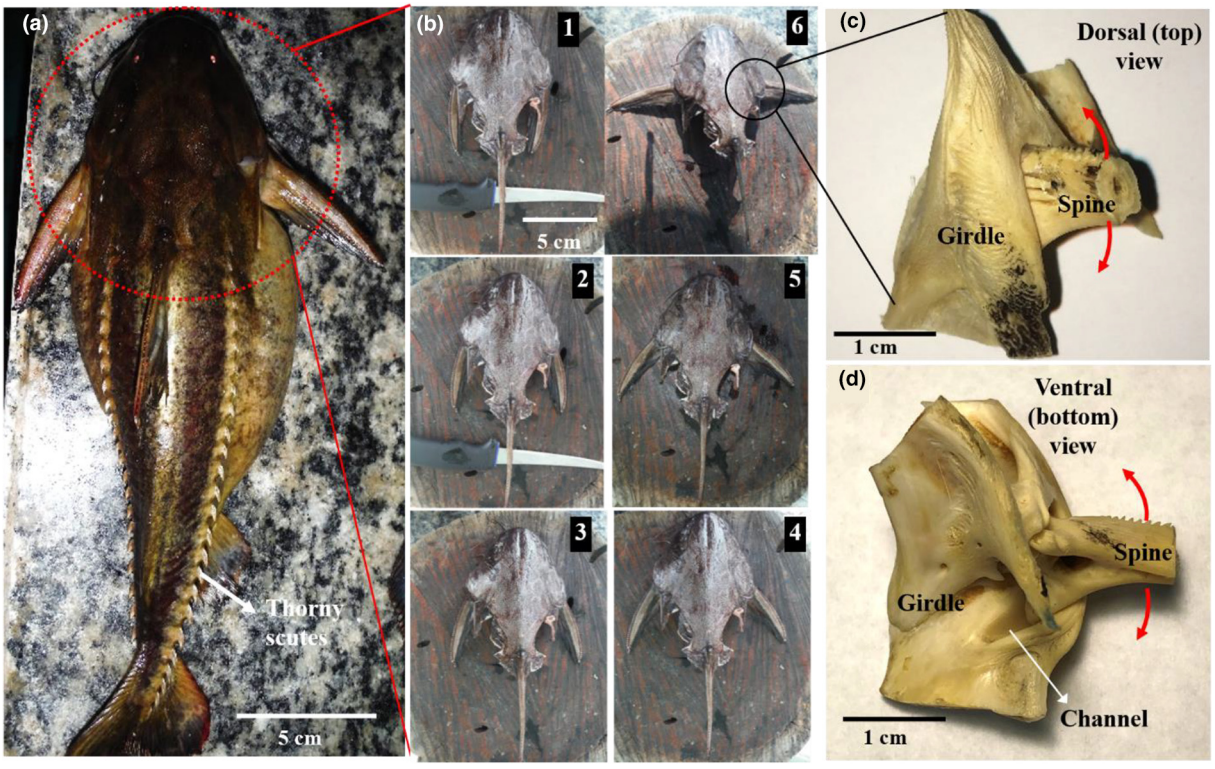

FIGURE 1

The locking phenomenon of the pectoral spines on the thorny catfish. (a) A thorny catfish (*Doradidae*) caught in the Paraguay River, Brazil. The pectoral spines are partially abducted and two arrays of scutes with hooked tips are located on both mid-lateral sides of the body. (b) Six locking positions of the pectoral spines are apparent just after the fish was decapitated. (c, d) Dorsal (top) and ventral (bottom) views of the skeletonized joint part of the pectoral spine articulated with the girdle in the locked position, respectively. Arrows indicate the rotation direction.

ized ridges (the brighter red color in the CT image indicates a higher degree of compactness) with honeycomb-like structural components, which serves to significantly increase the surface roughness of the channel wall.

The spine base is shown in Fig. 2e. There are several structural components on the bony base of the spine that are key: the anterior component (boxed and marked as A) and the dorsal component (boxed and marked as D). The detailed structure of these two key components are presented by the micro-CT images in Fig. 2f and 2 g, respectively. The anterior component (Fig. 2f) has an overall triangular-like geometry with numerous ridges and honeycomb-like structures on the surface. The dorsal component (Fig. 2g) is the largest of the structural components on the spine base; its outer surface is also very rough, with numerous similar ridges and honeycomb-like structural features. When the spine is fully deployed, the anterior and dorsal components on the spine base can tightly fit into the locking chamber and spinal channel, respectively, and their complementary geometry and contacted rough surfaces serve to generate two sources of friction, denoted as F_1 and F_2 in Fig. 2b and e. These factors all work together to lock the spine firmly in the deployed position. Evidence of this dual-friction-based locking mechanism is provided in Fig. 3.

Fig. 3 shows a micro-CT image of the entire joint part of the pectoral spine base with articulated girdle. For better demonstration, both the lateral view and ventral view of the joint in the fully retracted and deployed (locked) positions are presented in Fig. 3a and b, respectively. It is clear that the dorsal component slides in the spinal channel from the posterior to the anterior end and that this trajectory of movement is determined by the curvature of the channel. When the spine is fully deployed, its basal part is firmly locked by the interaction of structural components on both the spine base and girdle interior. Fig. 3c provides a close-up view of the anterior component. The triangular-like anterior component (A) fits into the cavernous locking chamber and the contacted rough surfaces of both parts generate significant friction to control the locking of the entire spine. Supplementary friction is generated by the dorsal component (Fig. 3d). A cross-sectional view indicates that the anterior end of the spinal channel forms a cam-like channel that envelops the dorsal component (D), with the surfaces of these two parts (Fig. 2d and g) working synergistically to provide a further source of friction to augment the locking of the pectoral spine. Thus, the component D

Based on the structural characterization above, the locking mechanism of the pectoral spine on thorny catfish is fully unraveled and illustrated in the schematic rendition in Fig. 4. The frictional parts and mechanisms are shown and this rendition makes it easier to comprehend the locking mechanism and positions. The spine is engaged and rotates in the circular segment of the spinal channel (fossa). Three positions are shown: retracted (Fig. 4a), intermediate (Fig. 4b), and deployed (Fig. 4c). The upper rendition corresponds to the view from the top (dorsal view); the lower rendition corresponds to the view from the bottom (ven-

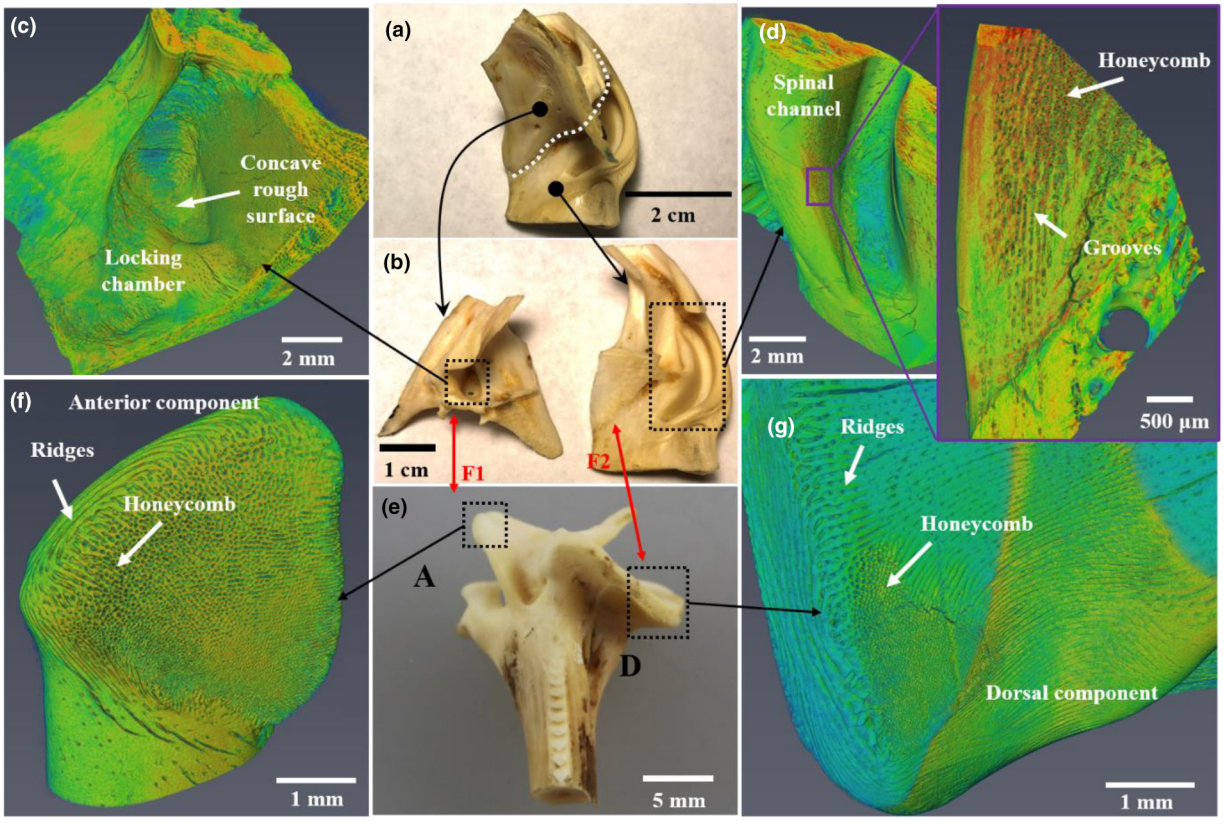

FIGURE 2

The structure of the girdle and spine base of the thorny catfish. (a) The isolated girdle part involved in the locking. The girdle is cracked along the dotted line and separated into two parts. (b) The separated two parts of the girdle. Two key structures are involved in the locking of the pectoral spines: one is a locking chamber boxed with dotted line on the left, the other is a spinal channel (fossa) boxed on the right. (c, d) Micro-computerized tomography (micro-CT) of the locking chamber and spinal fossa, respectively. The locking chamber has a concave structure and the inner surface is very rough. The spinal channel (fossa) is curved and its width narrows from the posterior end to the anterior end. The inner lateral wall of the spinal channel, shown in the inset of (d), is highly mineralized (brighter red color indicates higher mineralization) and is surrounded by grooves and honeycomb-like microstructures. (e) The basal part of the pectoral spine. There are several structural components on the base but two of them are the key components involved in the locking mechanism; these are the anterior component (A) boxed on the left and the dorsal component (D) boxed on the right. The locking of the pectoral spine relies on two sources of friction (denoted as F1 and F2) generated between these two key components. (f, g) Micro-CT of the anterior and dorsal components, respectively. (f) The anterior component has a triangular shape with ridges and honeycomb-like structures surrounding its surface. (g) The dorsal component is the largest component; its outer surface also has distinct ridges and honeycomb-like structures to enhance the roughness.

tral view). When the spines are fully retracted (Fig. 4a), the spine base is located at the posterior end of the spinal channel with adequate room for free movement, with no friction generated. When the spine is in the intermediate position (Fig. 4b), the dorsal component is engaged with the grooves and rough internal surface of the spinal channel generating a significant resistance force. When the spine is fully deployed (Fig. 4c), in addition to the engagement by the dorsal component and spinal channel, the anterior component (shown in the bottom part of Fig. 4b) fits into the locking chamber, resulting in a further locking mechanism that uses friction to ensure immobilization (with the spines deployed for protection).

This locking phenomenon of the pectoral spines is prevalent in most species of catfish [25,26]. To confirm the two-friction locking mechanism described above, the pectoral fin spines of the common channel catfish were also investigated with same techniques; details are provided in Fig. 5. It is evident from Fig. 5a that the pectoral fin spines of channel catfish have the same locking phenomenon; moreover, the skeletonized pectoral joint part indicates that the spine is articulated with a girdle in a similar manner to the thorny catfish described above (Fig. 1c). Additionally, the anterior (A) and dorsal components (D) are again the two key structural components responsible for the locking mechanism. Micro-CT combined with scanning electron microscopy (SEM) images in Fig. 5 display this locking mechanism for the channel catfish; the fully retracted and deployed states are presented in Fig. 5b with the ventral (bottom) view of the deployed spine joint given in Fig. 5c. The locking mechanism again involves two sources of friction generated from (i) the anterior component with the locking chamber in the girdle (Fig. 5d) and (ii) the dorsal component with the ventrolateral wall of spinal fossa (Fig. 5e). More details of the locking mechanisms of channel catfish are provided in Fig. S1 in the supplementary information.

There are, however, some noticeable differences between the fully deployed (locking) state and the partially deployed (constrained) state. In the partially deployed state, the dorsal component can contact the ventrolateral wall of spinal channel only

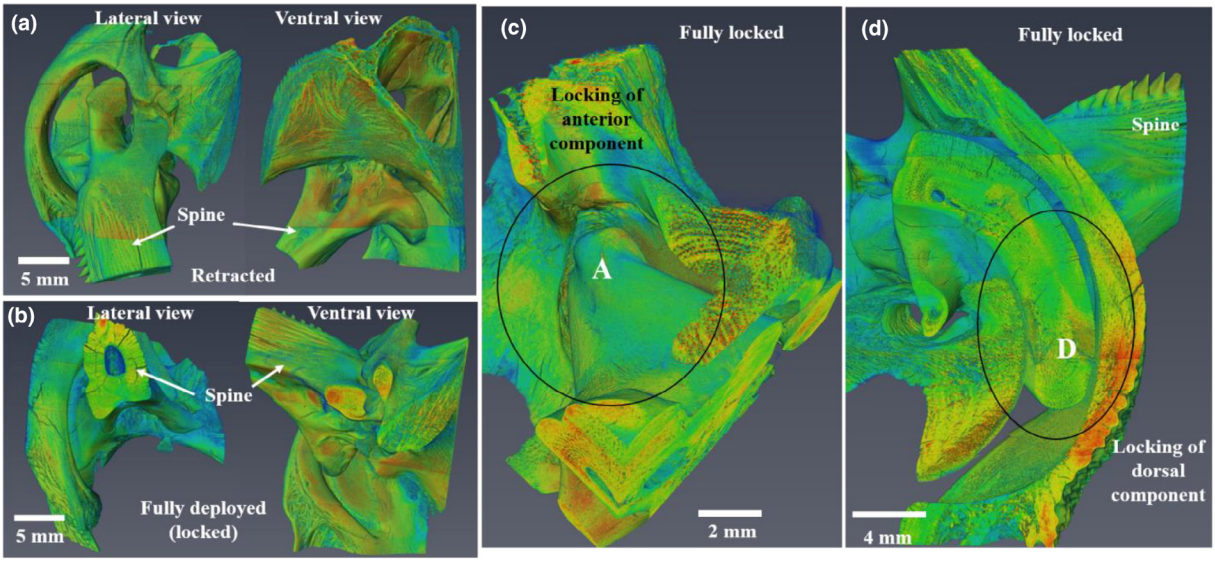

FIGURE 3

Micro-CT of the pectoral spine joint part revealing the locking mechanism for the thorny catfish. (a, b) The spine articulated with the girdle in the retracted state and fully deployed (locked) state, respectively. The lateral and ventral view of the joint are shown in both states. The dorsal component slides in the spinal channel during the deploying movement. The curvature and gradient width of the channel guide the movement of the spine base. (c) A close-up view of the anterior component (A) in the fully locked position. When the spine is fully deployed and locked, the anterior component (A) tightly fits into the locking chamber on the girdle. The complementary geometry and rough surface create significant friction to firmly lock the spine. (d) The cross-section of the dorsal component (D) in the locked position. With the spine fully lifted, the dorsal component slides into the anterior end of the spinal channel, where the width of the channel is about the same size as the dorsal component, resulting in a firm contact between the channel wall and outer surface of the dorsal component. The surface features on both parts, presented in Fig. 2(d) and (g), generate further friction that supplements the locking of spine.

with appropriate torque applied on the spine; thus, the anterior component can contact the locking chamber, resulting in the generation of noticeable friction. This is also why in the skeletonized specimens, the constraint, *i.e.*, resisting force to prevent further movement of the spine, can only be detected with slight torsion applied. However, when the spine is fully deployed, it can be locked firmly without applying torque. This is due to the fact that, in this position, the dorsal component is located at the anterior, *i.e.*, narrowest, end of the spinal channel, which does not need external force to ensure that the contact is sufficiently tight. Additionally, the anterior component in this position fully wedges itself into the locking chamber with the two strong frictional forces generated simultaneously to lock the spine firmly without the need for any torsion. For a living catfish, a muscular force is needed to achieve such constraint to partially deploy the spine. Once the spine is fully deployed though, no further muscular action is required by the fish to lock it; muscular action is only needed when the threat has passed and a slight torque must be applied on each spine to release them back to the retracted position. Therefore, the locking phenomenon of the spines, including the constraint, is generated by combination of ingenious design of the articulation and well-timed, but minimal, muscular work [24].

Another interesting finding is that after repeated deployment and retraction movement of the spine in skeletonized specimens, the locking force gradually deteriorates until it no longer operates. This is due to the wearing of the surface features of all the structural elements after multiple friction events. Evidence is provided in Figs. S2–S5 in the Supplementary Information. The ridges and honeycomb structures that generate the surface roughness on the dorsal and anterior components, ventrolateral wall of the spinal fossa and the apron region of the locking fossa, are all worn out, which significantly reduces the frictional force and makes the locking mechanism non-functional. Nevertheless, this wearing effect which causes the deterioration of the locking mechanism does confirm that the spine locking process is controlled by the two-friction mechanism. However, the living catfish are able to keep their locking ability of their spines functional after countless abductive and adductive motions, simply when the spine base and girdle remains fully hydrated, which increases the deformability of the bones and thereby reduces the wear of the surface structures. Moreover, as bone continuously remodels in living animals, the damaged surface structures can be readily repaired, making the locking of spines a very robust active defense mechanism in the entire life of catfish.

Based on the previous literature [24–27] and our current investigation, the locking phenomenon of pectoral fin spines for various catfish species results primarily from a two-friction locking mechanism generated from the intricate articulation of spine base with the ingenious inner design of the girdle. To demonstrate this, we 3D-printed the spine and girdle parts based on our CT scans, as shown in Fig. 6 where the articulated spine is shown in the retracted and deployed states. A video demonstrating the structure and locking mechanism of the 3D-printed pectoral spine joint is provided in Movie S1 in the Supplementary Information.

Pectoral spines: dentations

A dissected pectoral spine from the thorny catfish is shown in Fig. 7a, with debris from the dermis (dark) covering it. Unlike

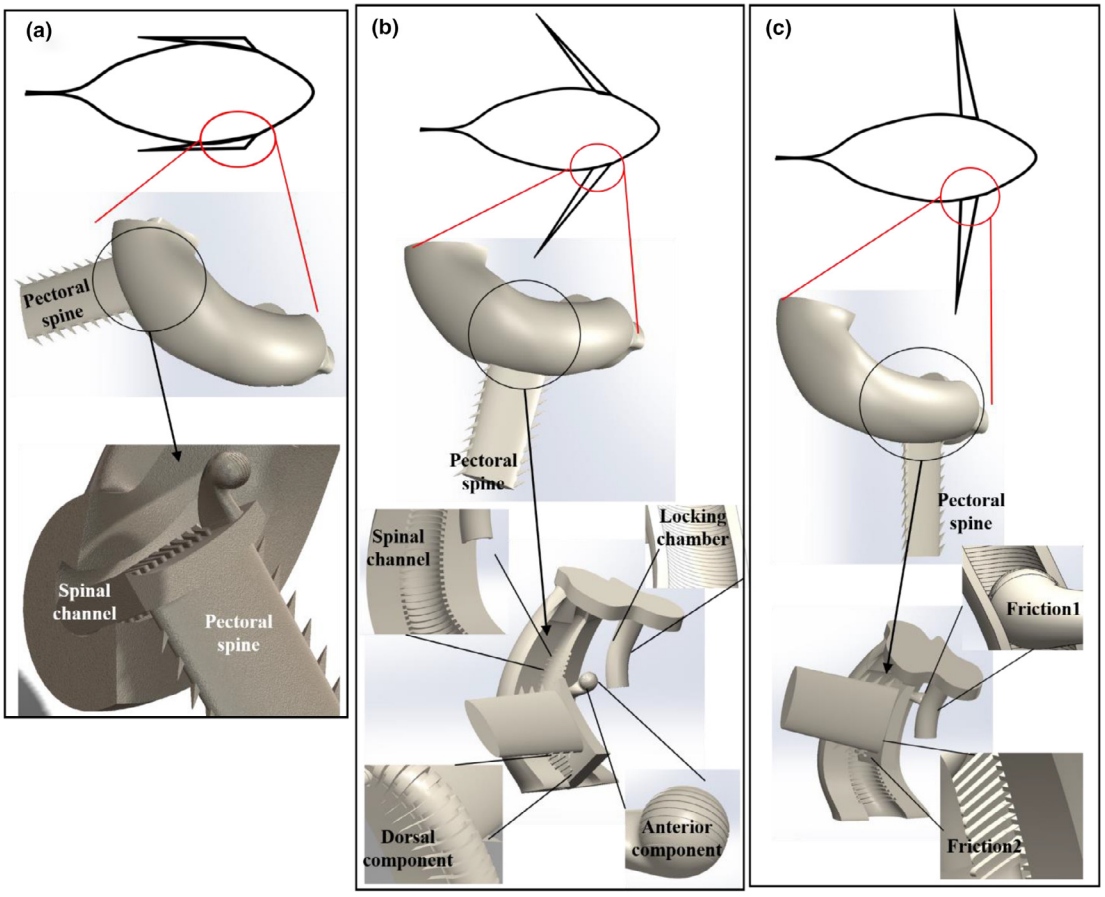

FIGURE 4

Schematic illustrations showing the two-friction based locking mechanism. (a) The spines are fully retracted, aligned with the longitudinal direction. The ventral view shows posterior end of the spinal channel is wide and there is no groove, causing no friction with the end of the spine. (b) The spines are partially deployed. The ventral (bottom) view of this position reveals all the components that lead to the friction-based locking: the spinal channel with grooves, the dorsal component with ridges, the locking chamber with a rough inner surface and the anterior component with ridges. In the partially locking position, the friction is already generated by the engagement of the spinal channel and dorsal component. (c) The spines are fully deployed and locked. The ventral view shows the two sources of friction which lead to the robust locking of the spines. They represent the friction generated between the spinal channel and dorsal component, and the friction generated by the locking chamber and locking tubercle on the anterior component. These two sources of friction are denoted as Friction 1 and Friction 2, in Fig. 2 (b,e).

the channel catfish, whose dentations only grow on the posterior side, the pectoral spines of thorny catfish have sharper and larger dentations that are rooted on both the anterior and posterior sides of spine (Fig. 7a,b,d and f). The alignment of the dentations on both sides of the fish are asymmetrical, which can improve the stabbing and cutting ability by promoting increased penetration and extraction damage in a predator's soft tissue. An interesting bifurcation in the alignment of the dentation orientations can be seen in the micro-CT images around the spine tip region (close to the distal end), as circled in Fig. 7b. The spine grows distally during the life of the fish (the distal end appears at first and the spine grows outward); such bifurcations demonstrate that this asymmetry is developed during the fish's maturity.

The center region of the spine is hollow (Fig. 7c, d) and the cavity is completely enclosed in a bony shell, forming a tubular structure. The diameter of the central cavity gradually decreases from the proximal (Fig. 7d) to the distal end (Fig. 7c), as the dotted-line circles indicate. Such a central hollow structure can be found in many other biological materials like bird feathers, beaks, and whale baleens, as it significantly reduces weight while maintaining flexure and buckling resistance. The sharp dentations on the catfish spines are highly mineralized with two distinct characteristics: (i) the mineralization gradually decreases from dentation tip to the base in the bony shaft, respectively colored in red and yellow in Fig. 7c and d; (ii) the mineral content is also associated with the alignment direction of the dentations, with higher mineralization always occurring on the outermost surface (Fig. 7e). The bifurcated dentation is an excellent example. Three neighboring dentations near the bifurcation are presented in the inset in Fig. 7e. Their cross-section, shown in Fig. 7e, demonstrates that for each dentation, the region close to the outer surface (red) has always higher mineralization than the inner side (green). The longitudinal cross-sections of the dentations close to the proximal end (Fig. 7f) confirm the trends in mineralization described above. Element mapping of one dentation, using energy-dispersive X-ray (EDX) spectroscopy (Fig. 7g), shows its composition to have high calcium and phosphorus

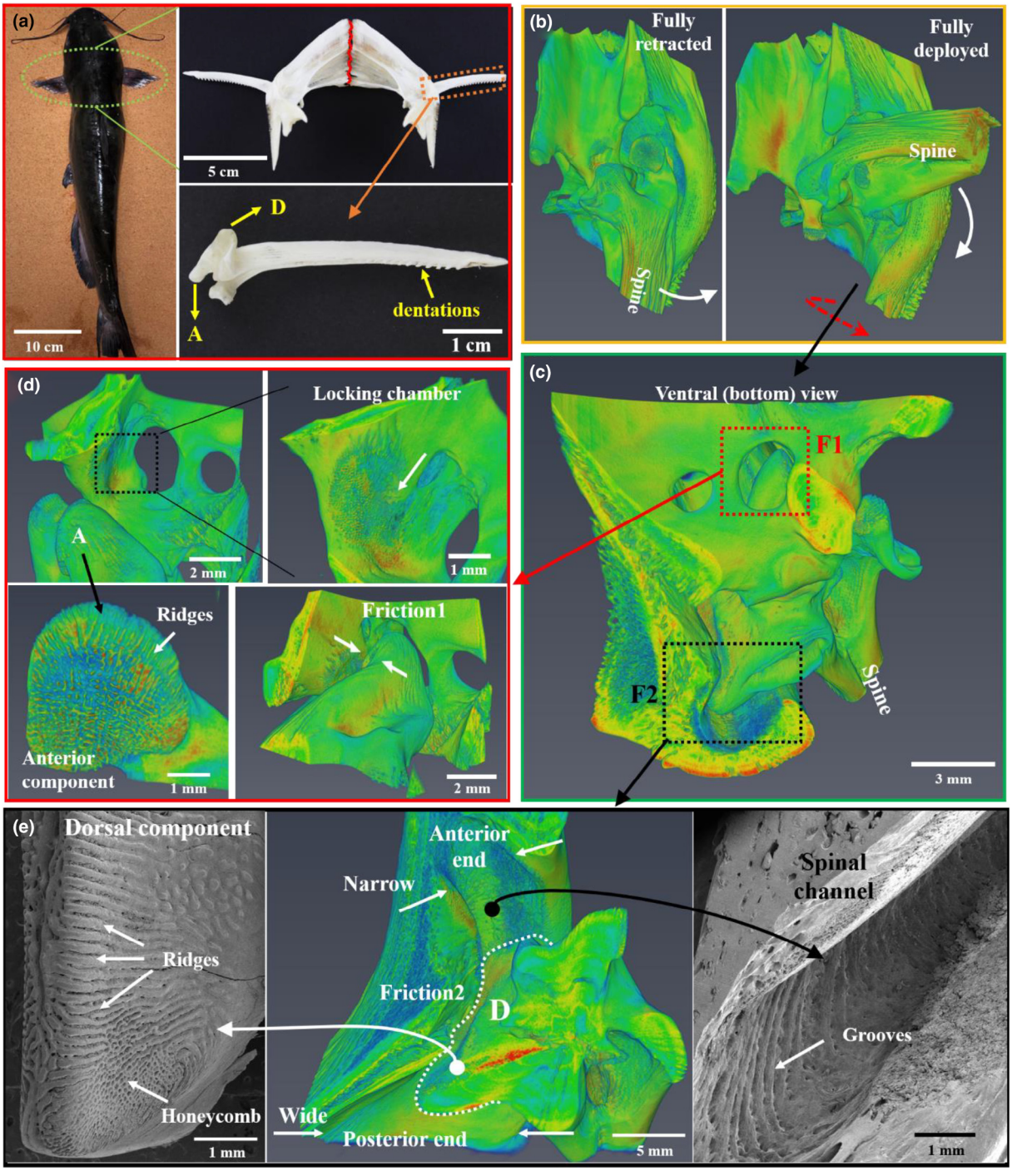

FIGURE 5

The locking mechanism of the pectoral spines on the channel catfish. (a) A channel catfish with the fully deployed pectoral spines. The skeletonized girdle articulated with spines is shown in the dorsal view. The girdle is composed of two symmetric parts which are sutured together, as the red line indicates. The isolated spine base also contains the two key structural components which provide the locking mechanism: the dorsal component (D) and the anterior component (A). There are numerous dentations scattered on the posterior side of the spines. (b–d) Micro-CT of the articulated spine and girdle. (b) The spine is fully retracted and deployed. (c) The joint in the fully deployed state is viewed from the ventral (bottom) side, which is the fully deployed state shown in (b) but rotated 90° clockwise, as the red arrow indicted. (d) The friction generated by the anterior component (A). The anterior component (A) has numerous ridges scattered on the surface. The locking chamber (squared with dot line) has a concave and rough surface. When the spine is fully deployed, the anterior component (A) becomes engaged with the concave locking chamber and as such generates frictional force (Friction 1). (e) The middle image is a micro-CT of the dorsal component (D) sitting in the spinal channel; the left and right images are scanning electron micrographs of the dorsal component and spinal channel, respectively. The spinal channel surrounds the dorsal component (D) and narrows anteriorly. Numerous ridges and honeycomb-like structures are on the surface of the dorsal component (D); additionally, the ventrolateral wall of the spinal channel is decorated with distinct grooves. The ridges on the dorsal component (D) tightly contact with the grooves of the channel wall, generating supplementary friction (Friction 2) to improve the overall locking of the entire spine.

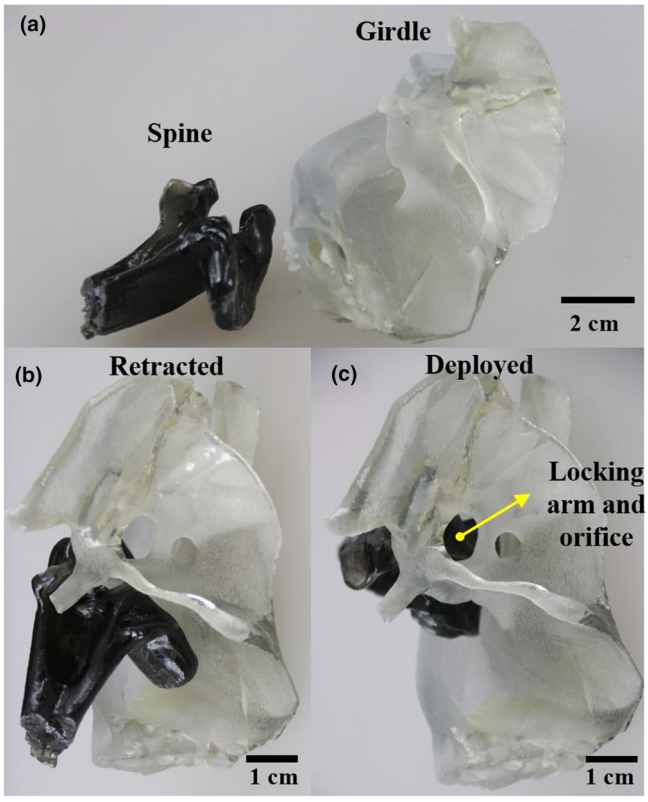

FIGURE 6

3D-printed pectoral spine joint. (a) A 3D-printed basal part of the pectoral spine (black) and girdle part (white) based on the micro-CT scan. The articulated spine in the (b) retracted and (c) deployed states.

contents but to be carbon deficient. The spine shaft is mainly composed of porous bone and the evidence is provided in supplementary Fig. S6.

To test the mechanical performance of the spine shaft, we performed compression stress–strain curves on the spine shaft as the inset in Fig. 8a shows. This shaft has a hollow structure inside with a shell composed of bone. The compressive stress–strain curves of four fully hydrated samples cut from this bony shell are presented in Fig. 8a, with the compression load applied along the longitudinal direction (marked by the arrows in the plot), as indicated in the inset. Results display a relatively large variation in the stress–strain curves, as the four samples were dissected from different regions of one spine shaft (along the longitudinal axis, from the proximal (Sample 1) to the distal end (Sample 4)). The average strength of four tested specimens was 97.2 ± 16.0 MPa, which is much higher than the strength trabecular bone (~5 to 10 MPa) but lower than that of cortical bone (~100 to 300 MPa), implying that the porosity in the bony spine shaft is between that of trabecular and cortical bone [28], since the these two figure is showing the center hollow cavity of the shaft, while we are talking about the porous structure in the shell of the shaft. The porous nature of the bony spine shaft is shown in Fig. S6c. The serrations and the plateau region after the yield point that can be seen in these stress–strain curves indicate that, like other bone-based tissues, the shell of the spine shaft has various crack-arresting mechanisms to prevent catastrophic failure after the initiation of a crack. These toughening mechanisms, which are generated at different length-scales, are depicted in Fig. 8b–f. In Fig. 8b, the major crack formed obliquely to the compression axis, indicating that failure is the result of shear stresses generated under the uniaxial compressive loading. Numerous secondary cracks were generated near this major crack (Fig. 8b, c), which serves as an efficient mechanism for dissipating stored elastic energy. Fibrillar bridging and pull-out behind the tip of secondary cracks reveals that the collagen fibrils are stretched during crack advance. These extrinsic toughening mechanisms [29] act to shield the crack tip by reducing the local stress intensity, thereby enhancing resistance to cracking. Similar toughening mechanisms can be seen by the bridging of larger fibers of the major crack (Fig. 8d). This synergy of mechanisms, primarily fibrillar delamination, bridging and pull-out (Fig. 8f) act in concert at the micrometer scale to confer significant structural integrity and excellent damage tolerance to the catfish's spines. Further, their sharp dentations with graded hardness (Fig. 10b), located on strong and tough hollow shafts, make the pectoral fin spines effective light-weight structural materials with excellent mechanical performance, all of which serve as a powerful weapon to aid the thorny catfish in its defense against predators.

Mid-lateral hooked scutes

The other unique characteristic of thorny catfish (Doradidae), which distinguishes them from other armored catfish, are the two arrays of hooked scutes embedded in the dermis along both mid-laterals. One array of the scutes was dissected (Fig. 9a), with the micro-CT imaging shown in Fig. 9b–d. Unlike the assembly of many other fish scales or dermal plates [2], these scutes are connected without any degree of overlapping (Fig. 9a, b); however, their base terminates in fibers that increase the prehension are embedded in the muscle; this is an ingenious design to decrease stress concentrations. The proximal extremities of the scutes are curved (blue areas in Fig. 9d) to follow the curvature of the catfish and for better anchoring on its body (Fig. 9d), which significantly increases their stability. Cross-sectional views in Fig. 9c and d show that the scute tip is very solid with higher mineralization (shown in yellow); the porosity gradually increases from the central region to the base, where the mineralization is lowest (shown in blue).

The scutes display a layered structure which follows the contour of their outline, highlighted by the dotted lines in Fig. 9c; this is likely associated with the layer-by-layer deposition of minerals during the growth of the scutes. SEM images of the surface, after fracturing the scutes in liquid nitrogen, reveal additional details of this inner structure (Fig. 9e–j). The alignment of the minerals, implied in Fig. 9c, is confirmed in Fig. 9e. The base region of the scute is composed of porous bone (Fig. 9f), with the pore size varying from micrometers (Fig. 9h) to nanometers (Fig. 9j). The collagen fibrils, with a well-defined 67 nm *d*-spacing (Fig. 9i), are wound around the pores to form a supporting wall (Fig. 9g) but their arrangement in the solid region between the pores is more clearly random (Fig. 9j).

Accordingly, it is evident that these mid-lateral scutes serve as a supplementary weapon, in addition to the pectoral spines, to enhance the active defense mechanisms of the catfish.

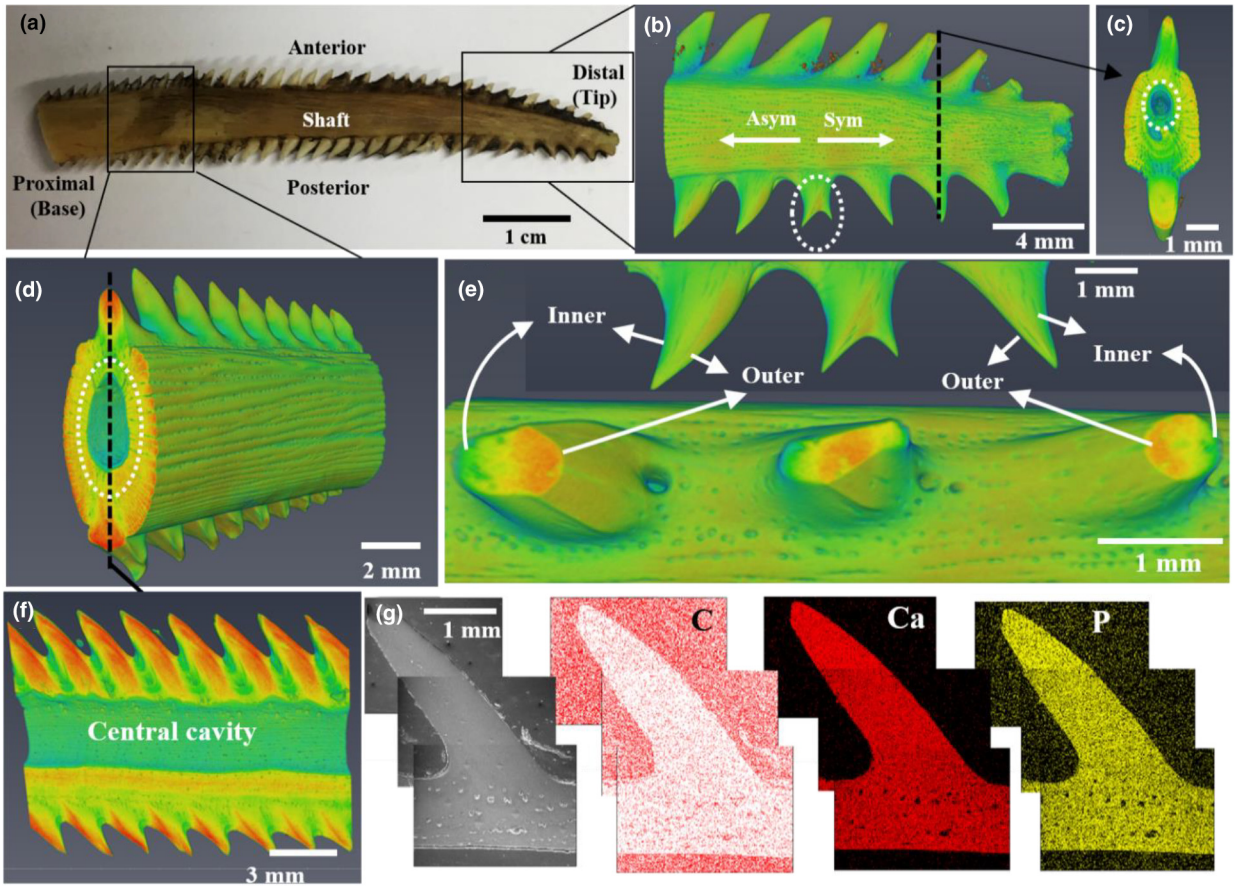

FIGURE 7

The structure of the pectoral spine of the thorny catfish. (a) The spine shaft is dissected from the right side. Numerous dentations are apparent on both the anterior and posterior sides asymmetrically. (b–f) Micro-CT of different regions of the spine. (b) Region close to the distal end of the spine reveals that there is a bifurcation in the directions of the pointed tips of the dentations on the posterior side, as circled by the dotted line. Bifurcation here means starting from the bifurcated point (circled), the dentations on distal side spike out symmetrically while on proximal side they point asymmetrically. (c) Transverse cross-section of the region close to the distal end shows that the central cavity (circled) is enclosed in the spine. (d) Transverse cross-section of the spine shaft closer to the proximal end shows a graded decrease in the mineralization from the dentations (red) to the bony shell (yellow), with the diameter of the central cavity (circled) larger than that in the distal region. (e) The cross-section of three neighboring dentations around the bifurcated one (also shown in inset) indicates that the region closer to outer surface (red) is always more mineralized than the inner region (green). (f) Longitudinal cross-section of (d) confirms the trends in mineralization: the dentations are more mineralized than the shaft and for each dentation its outer surface is more mineralized than its inner surface. (g) Scanning electron micrograph (SEM) of the cross-section of an isolated denticle showing element mapping of carbon, calcium and phosphorus.

Stridulation

Thorny catfish (Doradidae) are also called "talking catfish" because of their ability to produce a stridulatory sound by moving their pectoral spines. This noise generation mechanism is created by the same structures which cause the locking phenomenon [30]. During each sweep of the pectoral spine, the ridges on the dorsal component rub against the rough surface of the spinal channel and consequently generate a series of pulses which produces a characteristic sound. Previous research [24–27,31–34] quantitively identified that the channel catfish can also produce stridulatory sounds by moving its spines; the sweep duration is defined by how far the spine moves through the spinal fossa with each pulse duration determined by the thickness of each ridge on the base of spine and how long each ridge is in contact with the spinal fossa's surface [3]. Many creatures can produce under water sounds via extrinsic sonic muscles such as swim bladder sounds, but the stridulatory sound is unique to the catfish. Different from the drumming sounds generated by the swim bladder which serve as intraspecific communication, the stridulatory sounds are produced by the thorny catfish to target predators in interspecific communication to act as a warning [19,21,33].

Gradient structures for increased toughness

Liu et al. [29] systematically investigated the importance of structural and compositional gradients in biological materials. They are an important structural design element as pointed out by Naleway et al. [35]. These structures enhance the resistance to fracture while ensuring a high hardness in the surface, needed for cutting the predator. The two structures investigated here have indeed a clearly defined gradient in hardness. Fig. 10 shows the sections and hardness variation inside the spines sand scutes. The hardness varies from HVN 10 to 50 throughout the material. The highly mineralized dentations are hard but still exhibit some

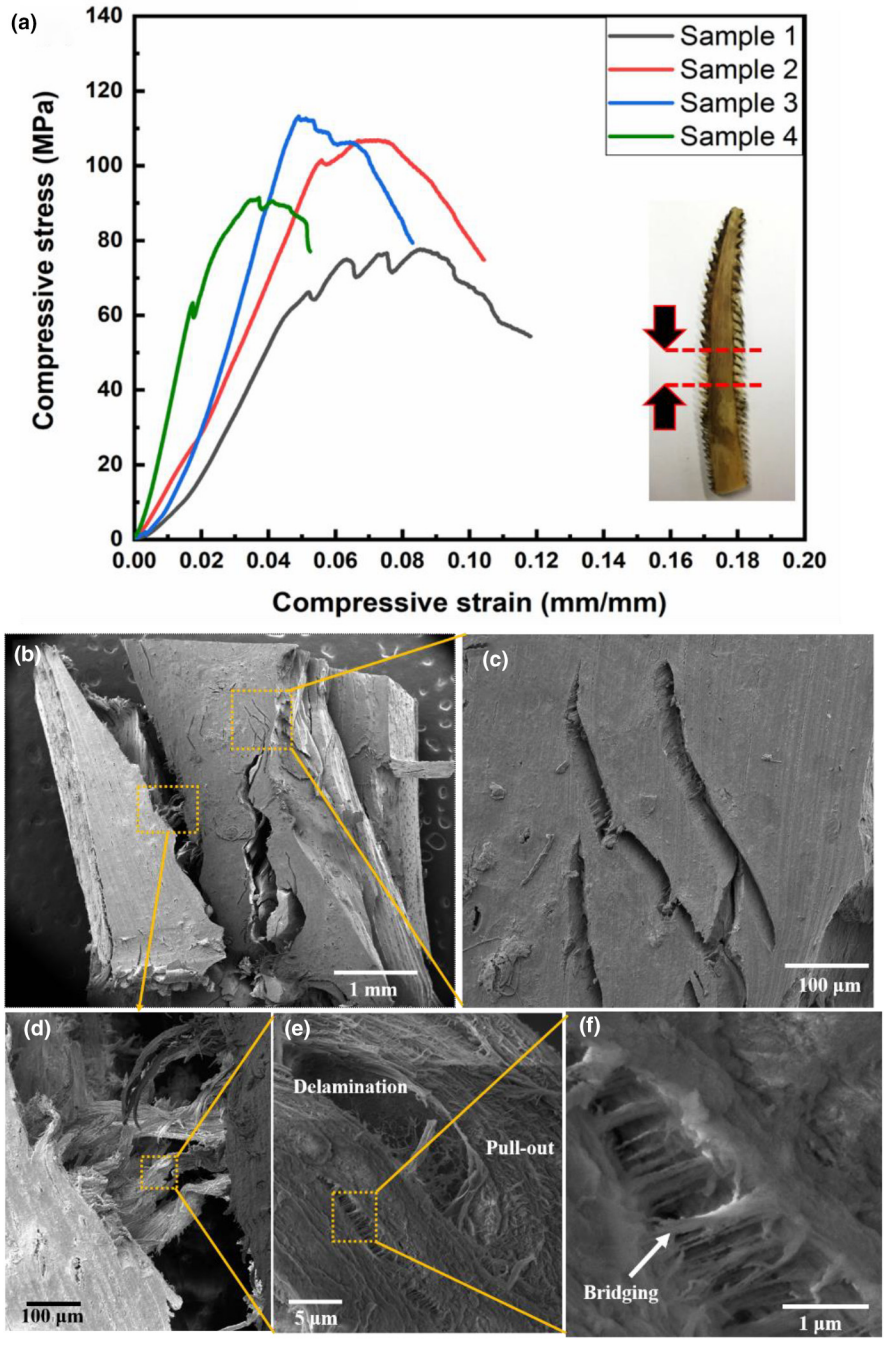

FIGURE 8

Compression testing and failure surface characterization of the spine of the thorny catfish. (a) Compressive stress–strain curves for the spine shaft. The compression direction is shown in the inset. (b–g) SEM images of a representative section after compression failure. (b) The oblique cracks indicate that the failure results primarily from the shear force. (c) Numerous secondary cracks are observed around the major crack. (d) Mineralized fibers can be seen to be still bridging the major crack after shear fracture. (e) Delamination, pull-out and bridging of the collagen fibrils on the crack-bridging fibers. (f) Close-up view of the mechanism of crack bridging due to intact collagen fibrils.

ductility, especially in the hydrated state. This is shown by the absence of cracks in the indentation corners, shown in Figs. S.7 and S8.

The spines are not only sufficiently strong for inflicting damage to a predator but are also quite tough due to their substantial deformability. A Vickers microhardness map on the longitudinal cross-section of one of the dentations with a bony base in Fig. 10b reveals that it gradually decreases from the tip (HVN ~ 50) to the porous bony base in a clearly graded fashion. The hard dentation tip provides high hardness and stiffness for penetrating a predator's tissue whereas the soft porous bony base confers a degree of flexibility and toughness to absorb excessive energy, all while maintaining a low weight. Akin to the strategy adapted in many other biological materials, the gradient transition in hardness between serves to reduce the internal stress and enhance stress redistribution, resulting in an increase in

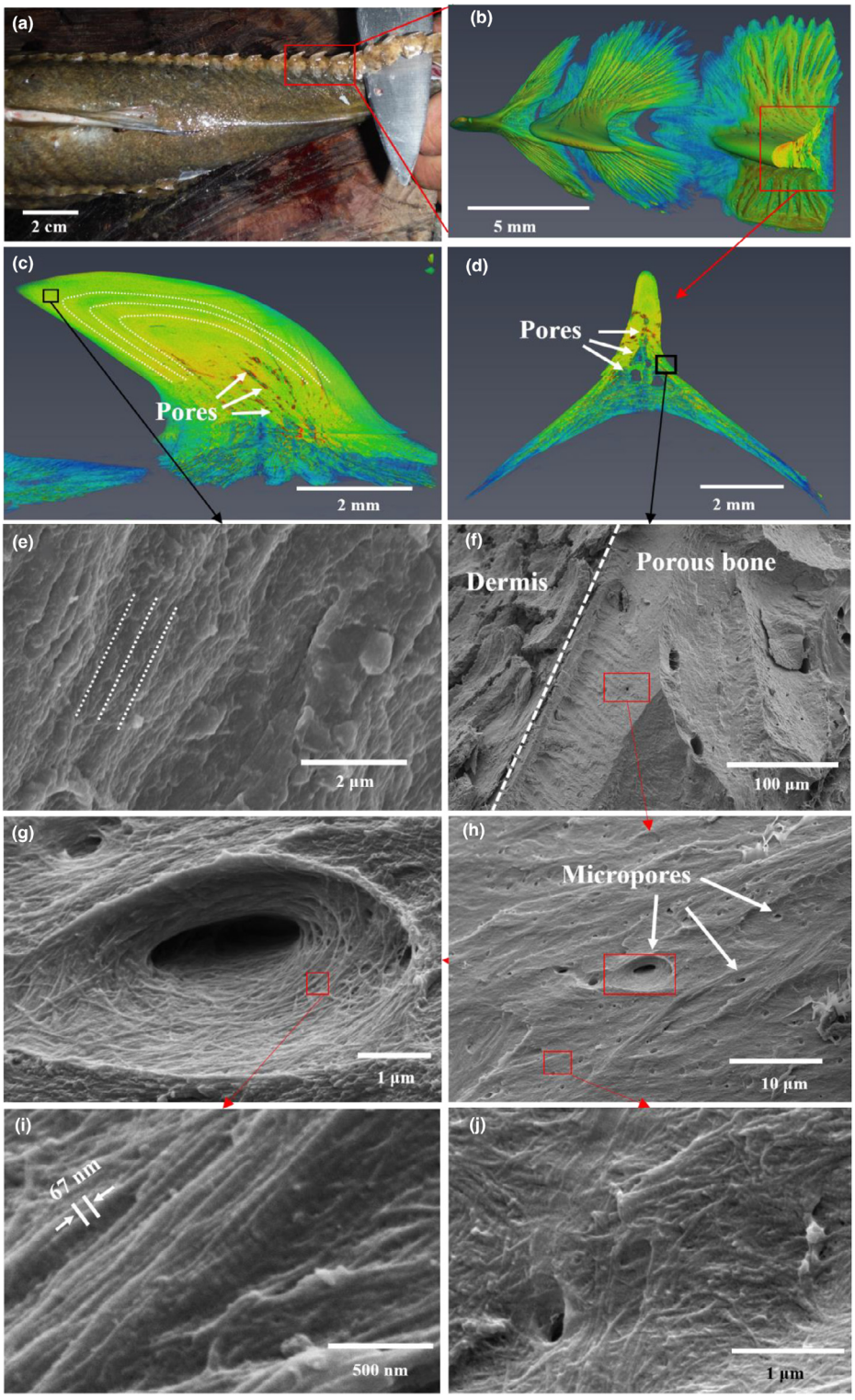

FIGURE 9

The structure of the mid-lateral scutes of the thorny catfish. (a) There are two sets of scutes with a hook shape sitting at the mid-lateral location on both sides of the thorny catfish. (b–d) Micro-CT of the scutes. (b) The scutes are connected without overlapping. (c) A longitudinal cross-section shows the scute tip to be highly mineralized (yellow-red) with the degree of mineralization gradually decreasing to bony base (yellow-green-blue). In contrast, the porosity gradually increases from tip to base. Contour lines of the mineral distribution are indicated by the dotted lines. (d) A transverse cross-section reveals that the wide curved base helps the scute to be anchored on the fish body. (e–j) SEM images of the cryo-fractured scutes. (e) The fracture surface of the tip region indicates that the mineral is deposited along the direction of the dotted lines, consistent with the observation in (c). (f) The porous bony base is covered by debris of the dermis. (g) Collagen fibrils wind around the pores forming the wall. (h) The pore size varies from nanometers to hundreds of micrometers. (i) The characteristic 67 nm *d*-spacing of the mineralized collagen fibrils. (j) The fibrils orient more randomly in the regions between the pores.

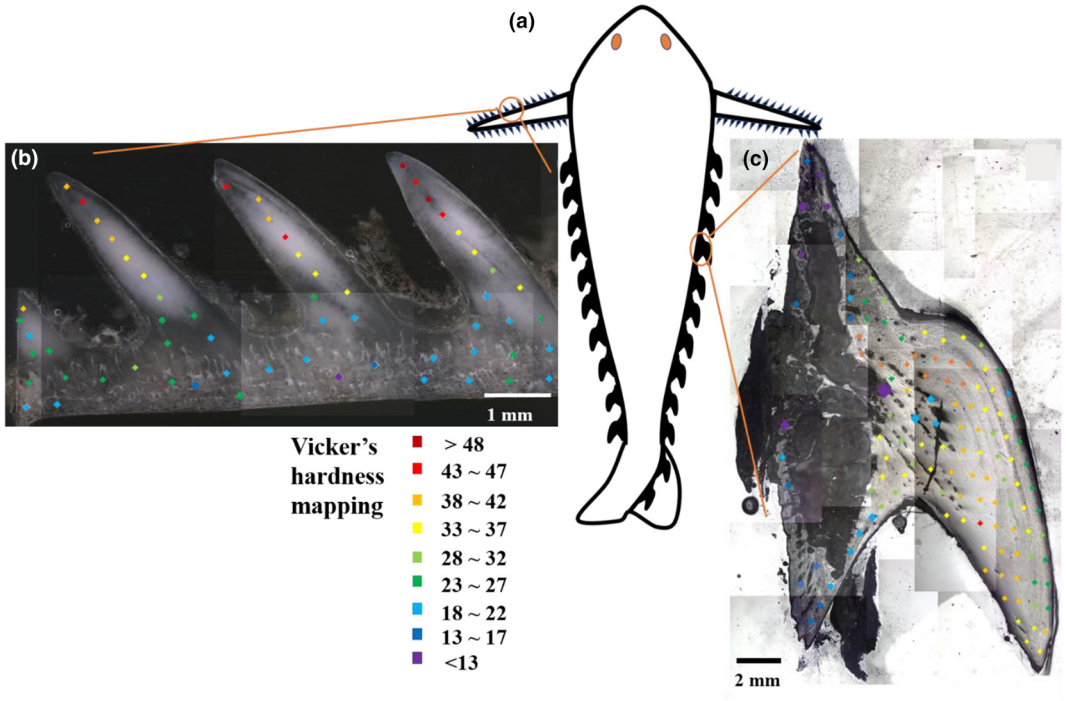

FIGURE 10

Gradient structure and hardness of spines and scutes. (a) Schematic drawing of a thorny catfish with deployed pectoral spines (and twisted tail). (b, c) Vickers microhardness mapping on a longitudinal cross-section of spine and scute; values gradually decrease from the sharp tips to base. Hardness of spine tip higher (VHN >48) than scute tip (VHN ~33–37).

the interfacial toughness [29,35,36]. SEM images of an indent on the dentation (Fig. S7), circled in Fig. 10b, suggest a degree of deformability in the highly mineralized dentation as no cracks are formed at the corners of the hardness indents, a common event in ceramics.

The gradient structure also generates varying mechanical properties across the scute (Fig. 10c). Hardness mapping indicates that the scute tip and central region have higher hardness values (HVN ~33–37) which gradually decrease toward the porous base (blue to purple). The contour lines of the alignment of the mineral are also visible in Fig. 10c, consistent with the observations in Fig. 9c. No recognizable cracks could be seen to have formed at the corners of the well-defined microhardness indents (Figs. S8), which indicates that the scutes display some ductility despite their hardness. Indeed, through their ingenious structural design and gradient properties, these hooked scutes can cut into soft tissue with their sharp hard tips yet can accommodate the excess deformation and delocalize the locally high stresses with their softer and porous base connected to the muscle.

Conclusions

Based on structural characterization and mechanical testing, we have attempted to reveal the active defense mechanisms of the armored (thorny) catfish, which specifically rely on two potent tactical weapons. These are summarized as follows:

1. *The sharp pectoral spines*. The unique pectoral spines of the thorny catfish can be partially or fully locked under threat and thereby provide defensive protection through their deployed structure. The locking mechanisms are generated by two sources of friction: that generated by the dorsal component and spinal channel, combined with the friction generated by anterior component and the locking chamber. Many catfish (Siluriformes) species have a similar mechanism as a mechanical active defense which expands their circumferential size to make them an unfavorable prey choice for predators. This locking mechanism is also associated with the stridulatory sounds produced by the catfish, which serve as a warning signal to contribute to their active defense.
2. *The mid-lateral scutes*. In addition to the lockable spines, thorny catfish also possess two arrays of mid-lateral dermal scutes with sharp hooks, which display potential cutting ability and provide a supplementary active defense capability.

In addition to the ingenious structural design of the articulation of the spine and the unique assembly pattern of the dermal scutes, the natural design over multiple length-scales of the material tissue of the catfish is extremely impressive, conferring excellent strength to the pectoral spines and mid-lateral scutes, yet with ductility and toughness, at a small weight penalty. The first element to this success is the hollow structure of the spine shaft, the central cavity of which is elongated along the axial direction, forming a tubular-like structure and enclosed in the bony shell. By moving the mass farther from the neutral plane, the flexure/buckling resistance of the spine shaft is significantly raised with no additional weight added, similar with the design strategies adapted in the feather rachis [37,38]. Finally, the use of gradient structures, *i.e.*, in the dentations on the spines and in the solid tip of the hook-shape scutes, provides flexibility and damage-tolerance in features designed as cutting tools to

inflict damage on the soft tissues of predators. To realize their functionality, the outer surface of the dentations and the tip region of the scutes are very hard due to a high degree of mineralization. However, the degree of mineralization and hence the hardness gradually decrease towards their softer base, to form a graded transition both in a graded transition in structural and mechanical properties.

By combining all these mechanical active defense mechanisms, the thorny catfish can successfully avoid becoming an easy prey to predators and as such has flourished in the various ecological environments in South America. We believe that such an intricate structural design with effective yet damage-tolerant materials can provide inspiration for the new light-weight structural materials and innovative robotics with gradient structures.

Methods

Materials

The thorny catfish (Doridiidae) was caught in the Paraguay River in Brazil; the channel catfish (Ictalurus punctatus) was purchased from Ranch 99 market in San Diego. The fish were decapitated after being euthanized in a freezer until spontaneous movement ceased. Pectoral girdles with spines were skeletonized with boiling water and oven dried at 60 °C. Scutes on thorny catfish were dissected with surgical blades and then air dried at room temperature.

Structural characterization

Direct observation of the articulations and movements of the pectoral spine relative to the girdle were based on manual manipulations of these skeletal preparations. All photographs were taken by cell phone (iPhone X) and digital camera (Canon 60D). The sectioning was performed with a diamond saw. Optical microscope characterization was conducted with Axio Fluorescence Microscope (Zeiss, German).

The micro-CT of the articulated spine with girdle and the dissected scutes for the thorny catfish was performed by synchrotron X-ray computed micro-tomography at beamline 8.3.2 of the Advanced Light Source synchrotron (ALS, Lawrence Berkeley National Laboratory) using standard procedures. The spine was located at the fully abductive and fully adductive positions, and both were scanned with a 1x lens with a voxel size of 9 μm. The scan for the scutes used a 2x lens with a voxel size of 4.5 μm. The micro-CT of the isolated spine shaft of the thorny catfish and the articulated spine with girdle of the channel catfish were conducted on air-dried samples in a Zeiss Versa 510 X-ray microscope (Zeiss, German) in National Center for Microscopy and Imaging Research (NCMIR). The voxel size for the scans of the channel catfish and the spine shaft of the thorny catfish was 3.6 μm and 1.8 μm, respectively.

Scanning electron microscopy (SEM) characterization and energy-dispersive X-ray (EDX) analysis were conducted with a FEI Quanta 250 microscope (FEI, Hillsboro, OR). The samples for SEM characterization were first immersed in the 2.5% glutaraldehyde for 1 h to fix the structure and then dehydrated with an ascending series of ethanols (30, 50, 70, 90, 95 and 100 vol.% twice). To obtain the oblique fracture surface, the scale was immersed in liquid nitrogen for 30 s and fractured using forceps immediately. All samples were dried with Tousimis Autosamdri 815B ((Tousimis, Rockville, MD) and then sputter coated with iridium using an Emitech K575X sputter coater (Quorum Technologies Ltd.) before observation.

Mechanical testing

Microhardness tests were performed on polished cross-sections of the dentations on the pectoral spine and mid-lateral scutes of the thorny catfish, using a LECO M-400-H1 hardness testing machine equipped with a Vickers hardness indenter and the applied load is 200 g with loading time of 15 s. Indent positions were recorded manually; the color scale for the microhardness was also created manually. The compression specimens were sectioned from the shell of the spine shaft and tested in an Instron 3367 testing machine (Instron Corp., Norwich, MA) at a strain rate of 10^{-3} s^{-1}. The specimens were all immersed in water for 24 h before testing to maintain their hydration. The failed specimens were immediately immersed into 2.5% glutaraldehyde solution to fix the morphology of the cracked region. The same dehydration procedure as the SEM sample preparation was performed on the fixed cracked samples prior to sputtering with iridium before final observation using FEI Quanta 250 (FEI, Hillsboro, OR) SEM.

3D-printing

The artificial catfish spine and girdle were fabricated by a commercially available 3D printer (Stratasys Objet350 Connex3). The materials utilized for printing consisted of a mixture of three polymers: a translucent photopolymer (TangoPlus FLX930), a flexible black photopolymer (TangoBlackPlus FLX980), and a rigid, clear photopolymer (VeroClear RGD810). The mixture ratio of these three materials was tuned to create different colors for the spine (black) and girdle (transparent white). A flexible, low-yield polymer (SUP705) was utilized as a support material. After the artificial structure was fabricated, the remaining support materials were removed by careful mechanical cleaning and washing with alkali solution.

Acknowledgements

This work was supported by the Multidisciplinary University Research Initiative to University of California Riverside, funded by the Air Force Office of Scientific Research (AFOSR-FA9550-15-1-0009), with subcontracts to UC San Diego and UC Berkeley. We appreciate Dr. Michael Tolley for kindly providing the 3D printer and the raw materials. We are also grateful to Ben Shih for his help with the 3D-printing. The Micro-CT scan for the spine shaft of armored catfish and the scan for channel catfish were conducted at NCMIR (National Center for Microscopy and Imaging Research), which is funded by a grant from the National Institute of General Medical Sciences of the National Institutes of Health (5 P41 GM103412). We thank Dr. Eric Bushong for help with the CT scanning and data analysis. We also appreciate the help from Melinda Lou on the hardness mapping of spine shaft. The authors also acknowledge the use of the X-ray synchrotron micro-tomography beamline (8.3.2) at the Lawrence Berkeley National Laboratory's Advanced Light Source, which is supported by the U.S. Department of Energy, Office of Science, Office of Basic Energy Sciences of the U.S. Department of Energy under contract no. DE-AC02-05CH11231.

Data availability

The help provided by my companions that participated in the Roosevelt Rondon Centennial Expedition, Cols. Hiram Reis e Silva, Ivan Carlos Angonese, Francisco Mineiro, Drs. Judith and Timothy Radke, as well as the Brazilian Army and the crew of the Calypso, is greatly acknowledged. We followed the trajectory of the 1914 Roosevelt Rondon Scientific Expedition [39] and the collection of specimens was an integral part of our endeavor, an official Flag Expedition by the Explorers Club. The raw data required to reproduce these findings are available from mameyers@ucsd.edu. The processed data required to reproduce these findings are available to download from [PERMANENT WEB LINK to be developed].

Appendix A. Supplementary data

Supplementary data to this article can be found online at https://doi.org/10.1016/j.mattod.2020.04.028.

References

[1] P.A. Abrams, Annu. Rev. Ecol. Sci. 31 (2000) 79.
[2] W. Yang et al., Adv. Mater. 25 (1) (2013) 31.
[3] Z.Q. Liu et al., Adv. Mater. 30 (32) (2018) 467.
[4] B. Wang et al., Acta Biomater. 41 (2016) 60.
[5] I.H. Chen et al., J. Mech. Behav. Biomed. Mater. 4 (5) (2011) 713.
[6] I.H. Chen et al., Acta Biomater. 28 (2015) 2.
[7] H.C. Quan et al., Adv. Funct. Mater. 28 (2018) 46.
[8] V.R. Sherman et al., J. Mech. Behav. Biomed. Mater. 73 (2017) 1.
[9] W. Yang et al., Acta Biomater. 9 (4) (2013) 5876.
[10] C.D. Derby et al., J. Chem. Ecol. 33 (5) (2007) 1105.
[11] R.G. van Gelder, J. Mammal. 49 (3) (1968) 576.
[12] D. Vandenspiegel et al., Biol. Bull. 198 (1) (2000) 34.
[13] D.S. Fudge, S. Schorno, Cells 5 (2) (2016) 25.
[14] D.C. Blackburn et al., Biol. Lett. 4 (4) (2008) 355.
[15] E. Heiss et al., J. Zool. 280 (2) (2010) 156.
[16] J.F.V. Vincent, P. Owers, J. Zool. 210 (1) (1986) 55.
[17] W. Yang et al., Acta Biomater. 9 (2013) 5297.
[18] W. Yang et al., Acta Biomater. 9 (2013) 9065.
[19] L. Knight, F. Ladich, J. Exp. Biol. 217 (22) (2014) 4068.
[20] B.T. Bosher et al., Ethology 112 (2) (2006) 188.
[21] L.S. Forbes, Oikos 55 (2) (1989) 155.
[22] J.J. Wright, J. Exp. Biol. 215 (11) (2012) 1816.
[23] J.L.O. Birindelli et al., Neotrop. Ichthyol. 9 (3) (2011) 515.
[24] M.L. Fine et al., Copeia 4 (1997) 777.
[25] E. Parmentier et al., J. Exp. Biol. 213 (7) (2010) 1107.
[26] J.S. Tellechea et al., Neotrop. Ichthyol. 9 (4) (2011) 889.
[27] M.L. Fine, et al., Catfish 2000: Proceedings of the International Ictalurid Symposium, Irwin, E.R., et al., (eds.) Amer Fisheries Soc, Bethesda, (1999), vol. 24, p. 105.
[28] D.R. Carter, W.C. Hayes, Science 194 (4270) (1976) 1174.
[29] Z. Liu et al., Prog. Mater. Sci. 88 (2017) 467.
[30] J.S. Nelson, Fishes of the World, fifth ed., Wiley, New York, 2007.
[31] M.L. Fine et al., In Conservation, Ecology, and Management of Catfish: The Second International Symposium, 2010, Michaletz, P.H., and Travnichek, V.H., (eds.) Amer Fisheries Soc, Bethesda, (2011), vol. 77, p 745.
[32] A. Heyd, W. Pfeiffer, Rev. Suisse Zool. 107 (1) (2000) 165.
[33] F. Ladich, Bioacoustics 8 (3–4) (1997) 185.
[34] T.L. Vance, Bios 71 (3) (2000) 79.
[35] S. Naleway et al., Adv. Mater. 27 (37) (2015) 5455.
[36] B.J.F. Bruet et al., Nat. Mater. 7 (2008) 748.
[37] T.N. Sullivan et al., Mater. Today 20 (7) (2017) 377.
[38] B. Wang, M.A. Meyers, Adv. Sci. 4 (3) (2017) 10.
[39] M.A. Meyers, River of Doubt: Reliving the Epic Amazon Journey of Roosevelt and Rondon on its Centennial, Create Space (2017).